Optical Engineering

OpticalEngineering.SPIEDigitalLibrary.org

Compact photonic triangular waveform generator with wideband tunability

Wenjuan Chen
Dan Zhu
Shilong Pan

SPIE.

Wenjuan Chen, Dan Zhu, Shilong Pan, "Compact photonic triangular waveform generator with wideband tunability," *Opt. Eng.* **57**(10), 106106 (2018), doi: 10.1117/1.OE.57.10.106106.

Compact photonic triangular waveform generator with wideband tunability

Wenjuan Chen, Dan Zhu,* and Shilong Pan*
Ministry of Education, Nanjing University of Aeronautics and Astronautics, Key Laboratory of Radar Imaging and Microwave Photonics, Nanjing, China

Abstract. A compact triangular waveform generator, consisting of a laser diode, a single dual-output Mach–Zehnder modulator (DOMZM), a variable optical delay line and a balanced photodetector (BPD), is proposed and experimentally demonstrated, using a single-frequency RF signal as the input. The DOMZM is biased at the quadrature point, so that no even-order harmonics of the RF frequency would be generated after the BPD. Then, the modulation index is properly selected to let the generated electrical first- and third-order harmonics approximately equal those of the triangular waveform. The use of the balanced detection not only increases the output power by 6 dB but also removes the DC component and the common-mode noise. No optical filtering is required, which guarantees the simplicity and wide frequency range of the system. A proof-of-concept experiment is carried out. Triangular waveforms with repetition rate tuning from 1 to 13 GHz are successfully generated, with the even-order harmonics suppressed by more than 54 dB. © *2018 Society of Photo-Optical Instrumentation Engineers (SPIE)* [DOI: 10.1117/1.OE.57.10.106106]

Keywords: microwave photonics; microwave waveform generation; electrooptic modulation.

Paper 172062 received Dec. 28, 2017; accepted for publication Oct. 2, 2018; published online Oct. 22, 2018.

1 Introduction

Due to the potential applications in optical signal processing, photonics-assisted triangular waveform generation has attracted great interest in recent years.[1–3] Previously, frequency-to-time mapping,[4,5] line-by-line shaping of the optical combs,[6] and self-convolution of a rectangular-shaped pulse[7] were applied to generate the triangular waveforms in the optical domain, but the duty cycle of the generated waveforms is not full, which greatly limits its application.[8] To generate the triangular waveforms with full duty cycle, approaches based on external modulation of a continuous-wave (CW) light were proposed,[9–18] in which the first- and third-order harmonics of the input RF frequency with a certain amplitude ratio are generated while the even-order harmonics are suppressed. To manipulate the optical spectrum for the generation of the desired electrical components, optical filters are always needed, which lead to limited frequency ranges and complicated structures.[9–13] To avoid the use of optical filtering, two RF signals with specific frequencies (f and $3f$),[14,15] or a dispersive element with predesigned dispersion[16] were applied, making the system sophisticated or frequency untunable. Photonics-assisted triangular waveform generation can also be implemented based on an optoelectronic oscillator, which eliminates the use of external microwave sources,[17–19] but the above limitations still exist. On the other hand, to evaluate the quality of the generated triangular waveforms, a parameter of root mean square error (RMSE) between the generated waveforms and the ideal ones is defined. For most of the schemes reported in the literature, only 30- to 40-dB rejection ratio of undesired harmonics is realized, leading to an RMSE value of around 2e-3 to 4e-3,[10,12,14,19] which needs to be further improved.

In this paper, we propose and experimentally demonstrate a compact triangular waveform generator using a single dual-output Mach–Zehnder modulator (DOMZM) driven by a single-frequency RF signal. Compared to the previously reported approaches, a super-large suppression ratio of the undesired harmonics can be easily realized by using a simple and compact structure composed of a laser diode (LD), a DOMZM, one RF source, a variable optical delay line (VODL), and a balanced photodetector (BPD). No optical filtering is needed to guarantee the simplicity and working frequency range. A proof of experiment is carried out. Triangular waveforms with frequency tuning range of 1 to 13 GHz have been successfully generated with the even-order harmonics suppression being larger than 54 dB, resulting in the RMSE between the measured waveforms and the ideal ones being smaller than 8.5e-4, showing an improvement with the quality of the generated waveforms.

2 Principle

The schematic diagram of the proposed microwave waveform generator using a DOMZM is shown in Fig. 1. A lightwave with an angular frequency of ω_0 generated by an LD is injected to the DOMZM. An RF signal of $V_m \cos(\omega t)$ with a frequency of ω and an amplitude of V_m is modulated at the DOMZM biased at V_{bias}. By injecting a time-delay difference τ between the two outputs of the DOMZM through the VODL, the two output signals of the DOMZM can be expressed as

$$\begin{cases} E_1 = (\sqrt{2}/2)^2 E_0 e^{j\omega_0 t}\left(e^{j\frac{\beta}{2}\cos\omega t + j\phi} + e^{-j\frac{\beta}{2}\cos\omega t - j\phi}\right) \\ E_2 = (\sqrt{2}/2)^2 E_0 e^{j\omega_0 t}\left[e^{j\frac{\beta}{2}\cos\omega(t+\tau) + j\phi} - e^{-j\frac{\beta}{2}\cos\omega(t+\tau) - j\phi}\right] \end{cases}, \quad (1)$$

*Address all correspondence to: Dan Zhu, E-mail: danzhu@nuaa.edu.cn; Shilong Pan, E-mail: pans@ieee.org

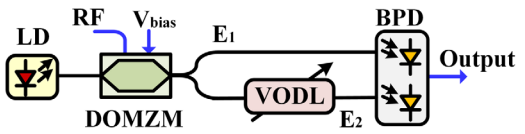

Fig. 1 The schematic of the proposed microwave waveform generator using a DOMZM. LD, laser diode; DOMZM, dual-output Mach–Zehnder modulator; VODL, variable optical delay line; BPD, balanced photodetector.

where E_0 is the amplitude of the optical carrier, $\beta = \pi V_m/V_\pi$, $\phi = \pi V_{\text{bias}}/V_\pi$, V_π is the half-wave voltage of DOMZM. The two outputs in Eq. (1) are then injected into the two optical ports of the BPD to realize the optical-to-electrical conversion. By setting the bias voltage V_{bias} to make $\phi = -\pi/4 + k\pi(k = 0, \pm 1, \pm 2\ldots)$, the output electrical current can be written as

$$\begin{aligned} I(t) &\propto E_1^* E_1 - E_2^* E_2 \\ &= \frac{1}{2}|E_0|^2[\sin(\beta\cos\omega t) + \sin(\beta\cos\omega(t+\tau))] \\ &= |E_0|^2 \sum_{n=0}^{\infty} (-1)^n J_{2n+1}(\beta)\{\cos[(2n+1)\omega t] \\ &\quad + \cos[(2n+1)\omega(t+\tau)]\} \\ &= |E_0|^2\{J_1(\beta)[\cos\omega t + \cos\omega(t+\tau)] \\ &\quad - J_3(\beta)[\cos 3\omega t + \cos 3\omega(t+\tau)] + \cdots\} \\ &= 2|E_0|^2\left\{J_1(\beta)\left[\cos\left(\omega t + \frac{\omega\tau}{2}\right)\cos\frac{\omega\tau}{2}\right]\right. \\ &\quad \left. - J_3(\beta)\left[\cos\left(3\omega t + \frac{3\omega\tau}{2}\right)\cos\frac{3\omega\tau}{2}\right] + \cdots\right\}. \end{aligned} \tag{2}$$

When $\omega\tau = \pm\pi/2 + 2k\pi$ (k is an integer), $\cos(\omega\tau/2) = -\cos(3\omega\tau/2)$, then Eq. (2) can be rewritten as

$$\begin{aligned} I(t) &\propto 2|E_0|^2\cos\frac{\omega\tau}{2}\left\{J_1(\beta)\cos\left(\omega t + \frac{\omega\tau}{2}\right)\right. \\ &\quad \left. + J_3(\beta)\cos\left(3\omega t + \frac{3\omega\tau}{2}\right) + \cdots\right\}. \end{aligned} \tag{3}$$

It can be seen from Eq. (3) that the output has only odd-order harmonics, and the ratio is approximately equal to those of the triangular waveform shown as

$$T(t) \propto \sum_{n=0}^{\infty} \frac{1}{(2n+1)^2}\cos[(2n+1)\omega t]. \tag{4}$$

Since the harmonics of a triangular pulse higher than the third-order have very small amplitudes and do not make a main contribution to the triangular waveform, only the first two Fourier components of a triangular pulse are considered.[9–16] By comparing the first two terms of Eq. (3) with Eq. (4), it can be seen when $J_3(\beta)/J_1(\beta) = 1/9$ and the harmonics higher than fifth-order are small enough to be ignored, a triangular waveform can be obtained. The relationship of $J_{2n+1}(\beta)$ ($n = 0, 1, 2, 3$) versus the value of the modulation index β is shown in Fig. 2. It can be seen that $J_3(\beta)/J_1(\beta) = 1/9$ can be realized when β is equal

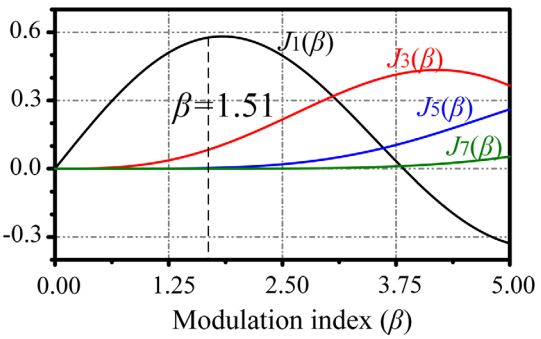

Fig. 2 The simulated curves of $J_1(\beta)$, $J_3(\beta)$, $J_5(\beta)$, and $J_7(\beta)$ versus the value of the modulation index β.

to 1.51. In addition, at this situation, the higher-order components, including the fifth- and the seventh-order harmonics, are small enough to be neglected.

As can be seen from Eq. (3), the proposed scheme can realize great suppression of the undesired even-order harmonics, which greatly improves the quality of the generated waveforms. The RMSE between the generated waveforms and the ideal ones is used to show the quality of the generated waveforms, being expressed as

$$\text{RMSE} = \sqrt{\sum_{i=1}^{N}\frac{(x_i - y_i)^2}{N}}, \tag{5}$$

where x_i and y_i are the amplitudes of measured triangular and the ideal one at the i'th sampling point, respectively, N is the total number of sampling points. A simulation is carried out to analyze the relationship between the RMSE and the rejection ratio of the even-order harmonics. Since the second-order harmonic is usually much higher than the other even-order harmonics and makes the major contribution, only the second-order harmonic is considered here to simplify the simulation. The RMSE values between the triangular waveforms with the second-order harmonic and the ideal ones without the second-order harmonic are shown in Fig. 3. It can be seen that the RMSE value decreases greatly with the increasing of the second-order harmonic suppression ratio. The RMSE value will be decreased by about 10 times when the second-order harmonic suppression ratio is improved by about 20 dB. When the second-order harmonic suppression ratio is 60 dB, the simulated RMSE is 5.73e-4. Thus, the proposed scheme will greatly improve the quality of the generated waveforms by realizing great suppression of the undesired harmonics.

3 Experimental Results and Discussions

An experiment based on the setup shown in Fig. 1 is carried out. A CW light at 1550.55 nm with a power of 10 dBm from the LD (TeraXion NLL04) is sent to the DOMZM (EOspace, AX-1x2-OMSS-20-PFA-SFA) with a bandwidth of 20 GHz and a half-wave voltage of 4.7 V. The modulated RF signal is generated by a microwave signal generator (Keysight N5183B, 9 kHz to 20 GHz). The VODL (General Photonics) has an optical delay range of 0 to 600 ps. The BPD (BPDV2150R-VF-FP) has a working bandwidth of 40 GHz and a responsivity of 0.53 A/W, respectively. The waveforms are observed by a digital sampling oscilloscope

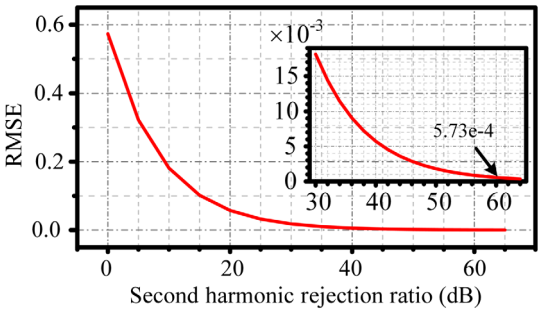

Fig. 3 The simulated relationship of the RMSE and the second-order harmonic suppression ratio.

(Agilent 86100C, 80 GHz). The optical spectra and the electrical spectra are measured by an optical spectrum analyzer (Yokogawa AQ6370C) with a resolution of 0.02 nm, and an electrical spectrum analyzer (R&SFSV40, 10 Hz-40 GHz), respectively.

First, a 5-GHz RF signal with a power of 17.1 dBm is modulated. By properly adjusting the time delay introduced by the VODL, an approximate triangular waveform will be obtained. The measured electrical spectrum and the corresponding generated waveform are shown in Figs. 4(a) and 4(b), respectively. As shown in Fig. 4(a), the third-order harmonic at 15 GHz is 19.1 dB lower than the fundamental component at 5 GHz. The ideal value is 19.08 dB, which corresponds to the amplitude ratio of 1/9 of the first two-term Fourier expansion of a triangular waveform. In addition, it can be seen that the even-order harmonics (the second- and the fourth-order) are suppressed by more than 60 dB, which is much higher than the results reported in previous works. The eye diagram of the observed waveform and the corresponding ideal triangular waveform are shown in Fig. 4(b), and the RMSE between the measured waveform and the ideal one is 6.815e-4, showing that the measured waveform fits well with the ideal one. The RMSE value is very close to the theoretically simulated value of 5.73e-4 shown in Fig. 3. Compared with the 30-dB even-order harmonics suppression ratio and the RMSE with value of 3.21e-3 realized in previous scheme,[14] the suppression ratio is improved by 30 dB, and the RMSE is reduced by an order of magnitude.

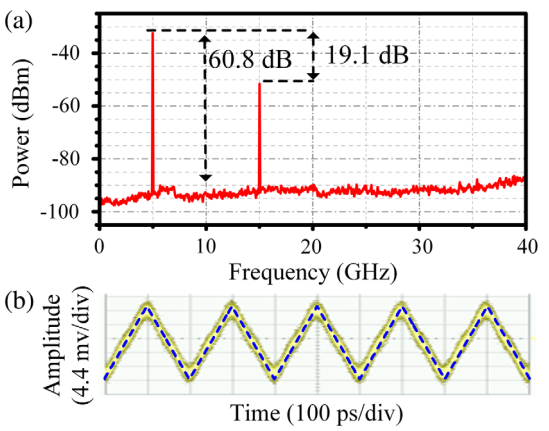

Fig. 4 (a) The experimental electrical power spectrum of the generated 5-GHz triangular waveform and (b) the eye diagram of the measured triangular waveform and the ideal one (blue dashed line).

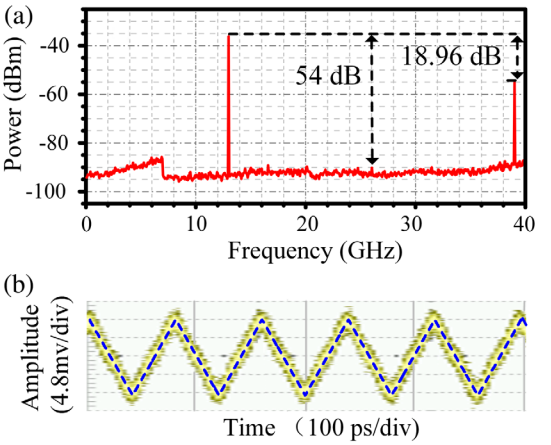

Fig. 5 (a) The experimental electrical power spectrum of the generated 13-GHz triangular waveform and (b) the eye diagram of the measured triangular waveform and the ideal one (blue dashed line).

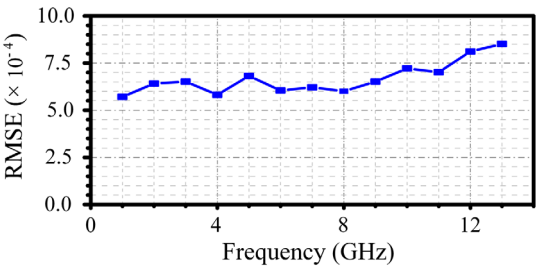

Fig. 6 The RMSE between the measured waveform and the ideal one at different frequencies.

To show the frequency tunability of the scheme, the frequency of the modulated RF signal is tuned from 1 to 13 GHz in a step of 1 GHz. By tuning the time delay introduced by the VODL correspondingly, triangular waveforms with repetition frequency from 1 to 13 GHz are successfully generated. For the 13-GHz working condition, the measured electrical spectrum and the waveform are shown in Figs. 5(a) and 5(b), respectively. The third-order harmonic at 39 GHz is 18.96 dB lower than the fundamental component at 13 GHz, which is also very close to the ideal value of 19.08 dB. The suppression ratio of the second-order harmonic is shown to be 54 dB, and the RMSE between the measured waveform and the ideal one is calculated to be 8.515e-4. The RMSE values between the measured waveforms and the ideal ones for different working frequencies are shown in Fig. 6, showing the good fitness between the measured waveforms and the ideal ones for the working frequency range of 1 to 13 GHz. It can be seen that for the proposed scheme, since no optical filtering is needed, thus the wide working frequency range is guaranteed, and the great suppression with the undesired harmonics is realized with a wide working range.

4 Conclusion

A photonic approach to generating full-duty triangular waveforms with undesired harmonics greatly suppressed is proposed and demonstrated. This scheme is simple and compact, using only an LD, an integrated DOMZM, a VODL, and a BPD. Neither optical filtering nor complicated structure is needed. The use of BPD removes the DC component

and the common-mode noise and also increases the output power by 6 dB. Triangular waveforms with working frequency range of 1 to 13 GHz are successfully generated, with the undesired even-order harmonics (the second- and the fourth-order) being suppressed by more than 54 dB, which guarantees the great fitness between the generated waveforms with the ideal ones. The scheme can be potentially applied in all-optical signal generation and processing systems.

Acknowledgments

This work was supported by the Fundamental Research Funds for Central Universities (NE2017002).

References

1. M. H. Khan et al., "Ultrabroad-bandwidth arbitrary radiofrequency waveform generation with a silicon photonic chip-based spectral shaper," *Nat. Photonics* **4**(2), 117–122 (2010).
2. A. I. Latkin et al., "Optical frequency conversion, pulse compression and signal copying using triangular pulses," in *European Conf. on Optical Communication (ECOC)*, pp. 1–2 (2008).
3. J. Chou, Y. Han, and B. Jalali, "Adaptive RF-photonic arbitrary waveform generator," *IEEE Photonics Technol. Lett.* **15**(4), 581–583 (2003).
4. J. Ye et al., "Photonic generation of triangular-shaped pulses based on frequency-to-time conversion," *Opt. Lett.* **36**(8), 1458–1460 (2011).
5. H. Y. Jiang et al., "Photonic arbitrary waveform generation based on crossed frequency to time mapping," *Opt. Express* **21**(5), 6488–6496 (2013).
6. B. Dai et al., "Generation of versatile waveforms from CW light using a dual-drive Mach–Zehnder modulator and employing chromatic dispersion," *J. Lightwave Technol.* **31**(1), 145–151 (2013).
7. Z. Wu et al., "Triangular-shaped pulse generation based on self-convolution of a rectangular-shaped pulse," *Opt. Lett.* **39**(8), 2258–2261 (2014).
8. A. I. Latkin et al., "Doubling of optical signals using triangular pulses,'' *J. Opt. Soc. Am. B* **26**(8), 1492–1496 (2009).
9. J. Li et al., "Frequency-doubled triangular-shaped waveform generation based on spectrum manipulation," *Opt. Lett.* **41**(2), 199–202 (2016).
10. W. Li, W. T. Wang, and N. H. Zhu, "Photonic generation of radio-frequency waveforms based on dual-parallel Mach–Zehnder modulator," *IEEE Photonics J.* **6**(3), 5500608 (2014).
11. X. K. Liu et al., "Photonic generation of triangular-shaped microwave pulses using SBS-based optical carrier processing," *J. Lightwave Technol.* **32**(20), 3797–3802 (2014).
12. W. L. Liu and J. P. Yao, "Photonic generation of microwave waveforms based on a polarization modulator in a Sagnac loop," *J. Lightwave Technol.* **32**(20), 3637–3644 (2014).
13. Y. S. Gao et al., "Photonic generation of triangular pulses based on phase modulation and spectrum manipulation," *IEEE Photonics J.* **8**(1), 1–9 (2016).
14. W. J. Chen et al., "Full-duty triangular pulse generation based on a polarization-multiplexing dual-drive Mach–Zehnder modulator," *Opt. Express* **24**(25), 28606–28612 (2016).
15. J. Li et al., "Photonic generation of triangular waveform signals by using a dual-parallel Mach–Zehnder modulator," *Opt. Lett.* **36**(19), 3828–3830 (2011).
16. J. Li et al., "Performance analysis of a photonic-assisted periodic triangular-shaped pulses generator," *J. Lightwave Technol.* **30**(11), 1617–1624 (2012).
17. T. W. Wu et al., "Simultaneous triangular waveform signal and microwave signal generation based on dual-loop optoelectronic oscillator," *IEEE Photonics J.* **8**(6), 7805610 (2016).
18. L. Huang et al., "Generation of triangular pulses based on an optoelectronic oscillator," *IEEE Photonics Technol. Lett.* **27**(23), 2500–2503 (2015).
19. W. Y. Wang et al., "Triangular microwave waveforms generation based on an opto-electronic oscillator," *IEEE Photonics Technol. Lett.* **27**(5), 522–525 (2015).

Biographies for the authors are not available.